ANALYSIS AND DESIGN OF CFRP GRIDS FOR REINFORCED CONCRETE

Charles E. Bakis [1], Suresh Pannala [1], Renata S. Engel [1], and Thomas E. Boothby [2]

[1] *Department of Engineering Science & Mechanics, 227 Hammond Bldg., The Pennsylvania State University, University Park, PA 16802, USA*
[2] *Department of Architectural Engineering, 104 Engineering Unit A, The Pennsylvania State University, University Park, PA 16802, USA*

SUMMARY: An analytical method was developed for simulating the tensile and pullout behavior of carbon fiber reinforced polymer (CFRP) grids used as reinforcement for concrete. Novel fiber placement patterns in the grids were explored. It was determined that increased proportions of curved fibers, i.e. fibers that provide continuity between the longitudinal and transverse elements of a grid, improves the pullout stiffness of the grid by increasing the shear stiffness of the grid near each joint. However, proportionally larger curved fiber content also degrades the through-joint tensile stiffness and strength of the grid. Excellent agreement between the model and experiments is demonstrated for the case of stand-alone tension loading. The modeling approach established in this paper enables the exploration of improved grid designs and also forms the basis of a more sophisticated model of a concrete structure reinforced with FRP grids.

KEYWORDS: grid, concrete reinforcement, analysis, design, manufacturing

INTRODUCTION

Fiber reinforced plastic (FRP) composite materials are attracting interest for their potential as high-strength, durable replacements of steel reinforcement in concrete structures. The durability advantage versus steel is especially apparent in chloride-rich environments such as near the ocean or where de-icing agents are used. Considering the time savings involved in construction using lightweight, pre-formed, two-dimensional FRP reinforcements, FRP grids also have a strong potential for near-term implementation in applications such as precast stay-in-place formwork, curtain walls, and decks [1].

Major performance parameters for reinforcement materials in concrete are tensile strength and bond strength, although stiffness also needs consideration for serviceability reasons (crack width and deflection in the structure). With FRP reinforcement, the anisotropic strength and stiffness properties as well as the geometry of the reinforcement control tensile *and* bond behaviors provided there is adequate concrete cover to eliminate failure of bond by failure of the concrete [2]. In the case of orthogonal, two-dimensional, FRP grid reinforcement, bond is achieved by mechanical interlock at the joints rather than continuously along the reinforcement as in unidirectional reinforcement bars. Hence, FRP grids must have

good through-joint tensile strength as well as good interlocking rigidity and strength at the joints.

The authors have previously reported experimental results of tensile and pullout tests of carbon fiber reinforced vinylester (CFRP) orthogonal grids with four types of fiber placement patterns [3-5]. In the first round of grids manufactured at Penn State University, tows of fiber were placed with various proportions of a cross-ply pattern, as is most often done commercially [1], and a staircase pattern where the tows turn at right angles at the joints (Fig. 1). The idea of the staircase pattern is to increase the mechanical interlocking stiffness and strength of the grid by virtue of fiber continuity between the longitudinal and transverse grid elements. Indeed, it was found that increased proportions of curved tows improved the stiffness and strength of mechanical interlock with concrete in direct pullout tests. The tradeoff, however, was decreased tensile strength and stiffness of the grids when tested outside of concrete.

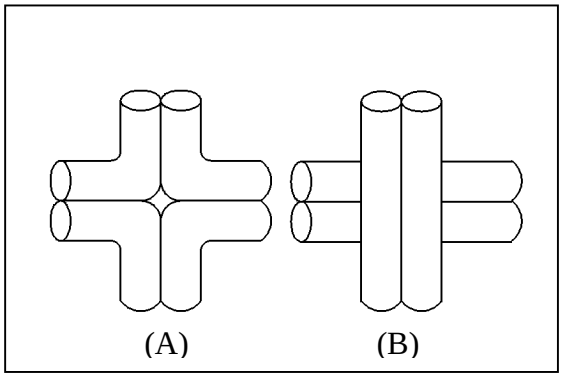

Fig. 1: Fiber placement patterns at a joint: type A, curved tows; type B, cross-plied tows [4]

At the time the four types of grids reported in Refs. [3-5] were designed and manufactured, it was not known exactly what the performance tradeoffs would be between cross-plied and curved tows in the joint region. Hence, the objective of the present investigation is to develop a means of modeling and analyzing the tensile and pullout behaviors of CFRP grids having various proportions of layers with cross-plied and curved tows in the joints. Test results from previously manufactured grids were used to verify the analysis. Having such a proven ability to analytically perform trade studies of tensile and pullout behaviors could save large amounts of fabrication and testing time in developing new, improved CFRP grids. Following verification of the analytical modeling approach developed in this paper, a second round of grids will be designed, manufactured and tested in future work.

MESOSTRUCTURE OF CFRP GRIDS

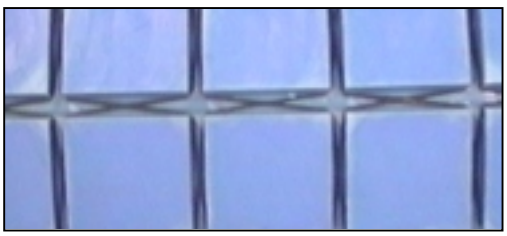

Fig. 2: Single layer of curved-tow pattern placed into female grid mold

Before explaining the modeling approach for CFRP grids, it is necessary to review the mesostructure of the grids themselves. Figure 2 shows the actual orientation of one layer of curved tows (type A in Fig. 1) after it has been placed in the flexible grid mold. Due to the tension maintained on the tows during placement, the curved tows cling to the corners of the mold and, therefore, promote the formation of resin-rich pockets at the center of the joint. Similarly, despite the application of a male mold to promote uniform compaction during hot-pressing of the grid [3-5], the corner regions containing curved tows tended to be slightly greater in thickness than the remainder of the grid due to the resistance of the tows to compaction at the corners. In the leg elements of the grid, the curved tows are oriented predominantly at about ±5-deg. versus the longitudinal (0-deg.) and transverse (90-deg. directions) following cure. The cross-plied layers (type B in Fig. 1) consist of tows simply

laid in the 0-deg. and 90-deg. orientations in the mold. In the experiments done previously, lay-ups of A/A/B/B/A/A, A/B/B/B/B/A, and B/B/B/B/B/B were used. These are referred to as 33%, 67%, and 100% cross-plied grid designs, respectively. Where the tows do not nest neatly, it is assumed that resin takes up the remaining space, thereby lowering the local fiber volume fraction. Such differences in fiber orientation and fiber volume fraction are accounted for in the model.

EXPERIMENTAL CHARACTERIZATION

Experiments were done previously to characterize the stand-alone tensile and pullout behavior of a single longitudinal element of each grid design (Fig. 3) [3-5]. In the tensile tests, the repeating unit stiffness was calculated by dividing the load by the center-to-center displacement between transverse elements. Grid strength, defined as the maximum load obtained during the tensile test, was based on complete separation of the grid segment and was characterized by fiber failure in or near or a joint. Pullout stiffness was computed by dividing the applied load by the displacement measured at the free end of the concrete block immediately following the onset of permanent slip. Pullout strength was defined as the maximum load obtained during the pullout test and corresponded to tensile failure of longitudinal fibers in the single embedded joint or slightly offset towards the loaded end.

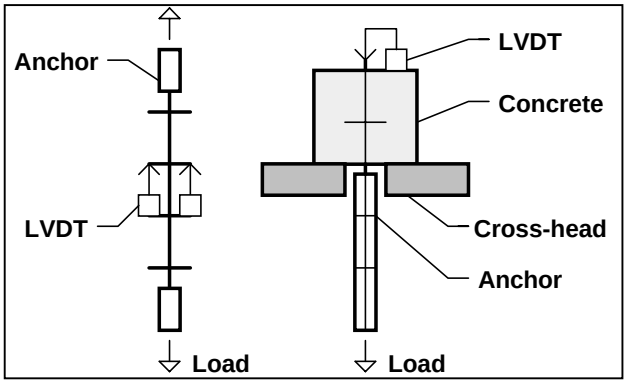

Fig. 3: Illustration of stand-alone tensile test (left) and pullout test (right) [4]

MODELLING APPROACH

Due to the complex shape and mesostructure of the CFRP grids, the finite element method was used to analyze tensile and pullout performance of the single longitudinal leg elements tested in the laboratory. A general-purpose finite element package known as ABAQUS[1] (version 5.7) was used in conjunction with the front-end processing capability of MSC/PATRAN[2] (version 6.2). One quarter of the area of the repeating unit centered on the joint was modeled (Fig. 4). Since symmetry allows modeling of only one-half the thickness, this model is referred to as the "one-eighth" model of a repeating unit. Longitudinal load was applied in both cases by a uniform longitudinal displacement boundary condition, δ, at the loaded end of the repeating unit.

For modeling the reactions in the stand-alone tension situation, longitudinal and transverse symmetry conditions were used (Fig. 4a). To model reactions in the pullout situation, the only symmetry that applies to the grid, besides the mid-thickness plane, is along the longitudinal centerline. However, computational limitations allowed only the one-eighth model to be used. Therefore, simplifying assumptions had to be made. It was first assumed that pullout resistance is accomplished by a combination of shear and bending actions at the connection between joint and transverse leg. Then, two types of boundary conditions

[1] Hibbitt, Karlsson & Sorensen, Inc., Pawtucket, RI, USA.
[2] MacNeal-Schwendler Corporation, Costa Mesa, California, USA.

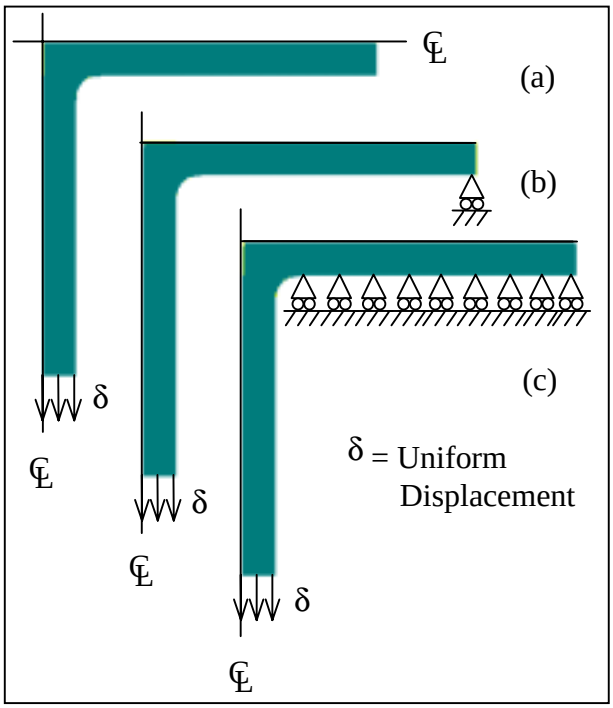

Fig. 4: One-eighth model of (a) stand-alone tension repeating unit, (b) pullout resisted by bending, (c) pullout resisted by shear

representing opposite extremes of physical constraints on the grid by concrete were selected. In the first pullout condition (Fig. 4b), the entire longitudinal load is resisted by a point constraint at the remote end of the transverse leg. In the second pullout condition (Fig. 4c), the longitudinal load is resisted by a vertically constrained leading edge of the transverse half-leg. The point and distributed constraints provide insight on the bending and shear resistances, respectively, of the connection between joint and transverse leg.

Type A (curved-tow) and B (cross-plied) layers were individually discretized with finite elements according the local fiber orientations and volume fractions determined in as-manufactured grids (Fig. 5). In the curved-tow layers, regions were modeled as either neat resin, curved fibers, unidirectional (5-deg.) fibers, or ±5-deg. angle-plied laminate. The corresponding angles on the transverse leg were relative to the 90-deg. global direction. In the curved fiber band, the volume fraction of fiber (V_f) was inversely proportional to the width of the band, varying from the 35% value remote from the corner to a fictitious 94% at the point of minimum bandwidth. The width of the curved band matched that measured on the actual grids and the fictitious fiber volume fraction was necessary to account for all the fibers present in the curved tow without needing to vary the local thickness of the tow as in the actual grid. The cross-plied layer has only two regions to discretize separately — cross-ply (0/90) and unidirectional (either 0-deg. or 90-deg. in the two legs). The model thickness is 3.18 mm and the other dimensions are given in Fig. 5. These dimensions are nominally identical to those of the as-manufactured grids.

Material properties within individual elements in all regions of each type of layer reflected the actual fiber concentrations and orientations in the grids. Layers were stacked in the model to resemble the lay-ups manufactured previously plus several other lay-ups not manufactured. Displacement continuity between the layers was enforced. Convergence of the solution was verified by halving the size of the elements until a <1% change in the overall stiffness of the model occurred. Two layers of elements through the thickness of each layer were found to be adequate for modeling purposes. The largest aspect ratio of the 6-noded triangular prismatic elements was approximately 4. Material properties in principal material coordinates are given in Table 1. Approximate values for unidirectional $(0)_T$ lamina properties in terms of volume fractions of constituents were calculated using the equations by Chamis [6]. Two-dimensional, in-plane transformation equations were used to obtain the 5-deg. off-axis material properties. The three-dimensional laminated plate analysis by Pagano [7] was used to obtain the out-of-plane properties of the (0/90) and (±5) laminated regions of the layers. These laminated regions were assumed to be symmetric about their local midplanes for element property calculations.

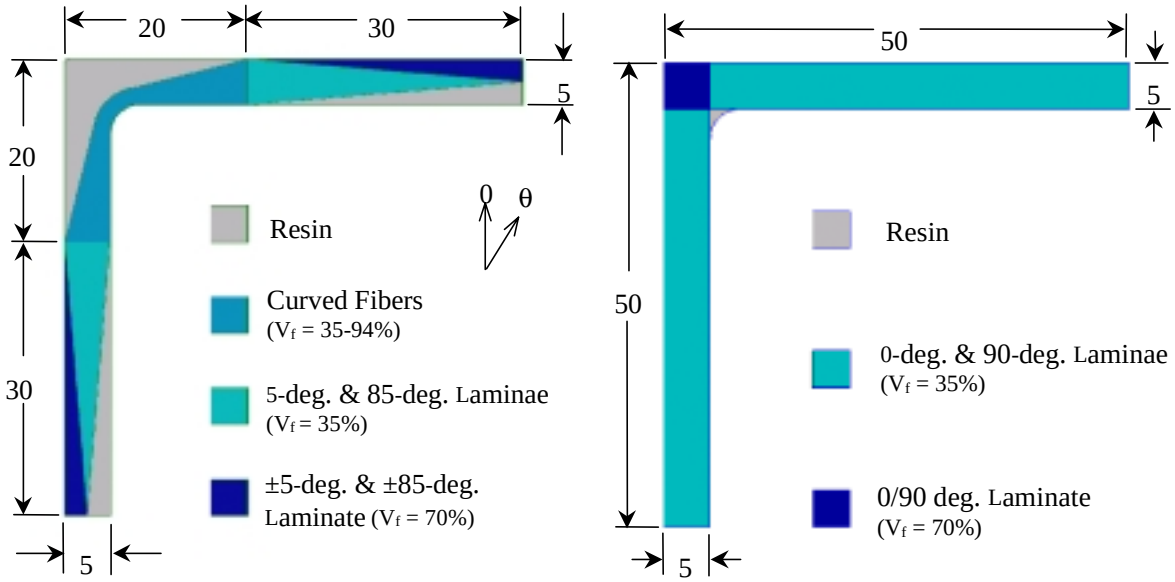

Fig. 5: Curved-tow layer (left) and cross-plied layer (right) as modeled by finite elements

Table 1: Assumed elastic properties of various regions of model

Region	Young's Moduli (GPa)[a]			Shear Moduli (GPa)[a]			Poisson's Ratio[a]		
	E_{11}	E_{22}	E_{33}	G_{12}	G_{23}	G_{13}	ν_{12}	ν_{23}	ν_{13}
$(0)_T$ V_f=35%	82.0	6.20	6.20	2.85	2.40	2.85	.27	.29	.27
$(\pm5)_S$ V_f=70%	158	9.29	9.27	6.53	3.65	5.42	.34	.27	.20
$(0/90)_S$ V_f=70%	85.1	85.1	9.87	5.44	4.36	4.36	.025	.28	.28
Curved	Varies according to V_f								

[a]1 and 2 refer to the major and minor in-plane axes; 3 refers to the out-of-plane axis.

The principal means of comparing the analysis to the experiments at this point of this investigation is the stand-alone tensile stiffness of the grid. In the analysis, the one-eighth model stiffness was transformed to a repeating unit stiffness of the actual grid by multiplying the end displacements by two and the applied load by four and re-computing stiffness in the usual manner. Equivalently, one could multiply the model stiffness by two to obtain the actual repeating unit stiffness.

RESULTS

The grid designs analyzed have the following percentages of cross-plied layers: 100, 90, 75, 67, 50, 33, and 25. Stiffnesses of tension and pullout models are compared first, followed by stresses in only the tension model.

Predictions of repeating unit tensile stiffness from the stand-alone tension analysis are shown in Fig. 6(a), along with the experimental results from the 100%, 67%, and 33% cross-ply grids. Clearly, the trend is a nearly linear decrease in tensile stiffness with decreased cross-plied layer content over the range studied. For cross-plied layer contents less than 20%, the decrease in stand-alone stiffness is expected to be much more dramatic due to the low stiffness of the remaining curved-tow layers. The agreement between the experimental data points and the model is quite good across the spectrum of grid lay-up patterns, indicating that

the tensile model was constructed with good assumptions and could serve well for design purposes.

Due to the limitations of the pullout model discussed earlier, it was not expected that the finite element results would correlate well with the experiments. Therefore, no comparison of stresses was attempted and the predicted pullout stiffnesses for different grid designs were only compared in a relative sense to each other. In the bending-dominated pullout model (Fig. 4b), the stiffness of each grid was normalized by dividing by the stiffness of the 100% cross-plied grid — 0.252 kN/mm). Likewise, the stiffnesses of the various grids in the shear-dominated model (Fig. 4c) were normalized by the 100% cross-plied value of 22.0 kN/mm. It is noteworthy that the normalizing factor for the shearing-dominated pullout stiffness is nearly two orders of magnitude greater than that for the bending-dominated pullout stiffness. This outcome underscores the dependence of overall pullout stiffness on the shear stiffness of the connection between joint and transverse leg. Figure 6(b) shows the predicted relative pullout stiffnesses of the various grid designs subjected to both boundary conditions. The shearing-dominated stiffness increases by nearly 30% as the curved-tow layer content increases from 0% to 75% of the thickness. The bending-dominated stiffness, on the other hand, decreases by about 40% over the same range of curved-tow layer content. The presence of curved tows therefore enhances the more important shear stiffness of the joint at the expense of the less important bending stiffness. In the experimental results reported in Ref. 5, it was noted that the pullout stiffness after the onset of permanent free-end slip increased with curved ply content. In those experiments, it was not possible to measure the elastic slip with the available equipment. The immediate conclusion to be drawn from the comparison of analysis and experiment is that the pullout stiffness of these grids is controlled by the in-plane shear stiffness near the joint.

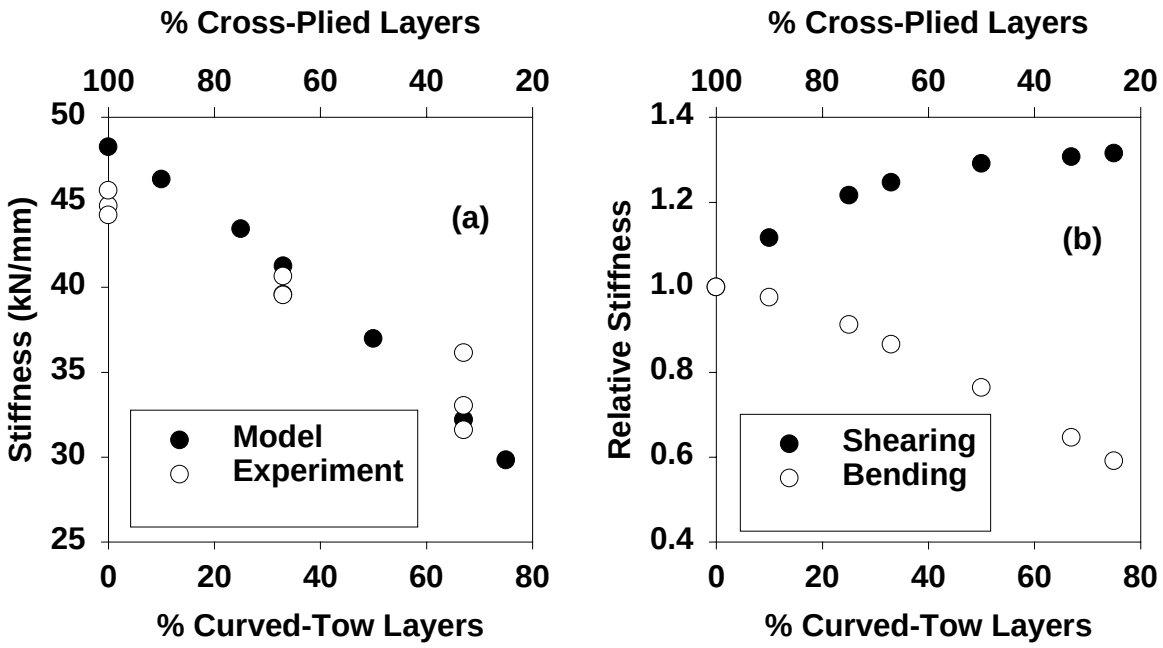

Fig. 6: Effect of joint design on (a) stiffness of repeating unit of stand-alone tensile model, with experimental comparisons; (b) stiffness of shearing- and bending-dominated pullout models relative to the 100% cross-ply design

In the experimental investigation [3-5], it was concluded that the fibers within the joint region of a grid are the critical element in the stand-alone tensile failure process. Little, if any, nonlinear or inelastic behavior was noted in the stress-strain data. This situation is easily

analyzed since subcritical damage modes and their local effects on constitutive behavior do not need to be included to obtain reasonable accuracy. To comparatively analyze the tensile load carrying capability of different grid designs, the recommended approach is to analyze strains in the various fiber directions in critical regions of the grids. Since fiber orientations vary throughout the grid, each layer was thoroughly searched for maximum fiber direction strains. The maximum fiber strains were divided by the remote, axial strain at the loaded end of the stand-alone tensile model to obtain a fiber strain concentration factor (K^f_ε). This factor can be used to compare the worst-case fiber direction strains in each grid design as a function of the applied strain. Strains were selected as the means of comparison rather than stresses since fiber volume content varies tremendously by position, making stresses impossible to compare.

The stress analysis results indicate that K^f_ε increases in the critical region of the cross-plied layers as the number of cross-plied layers decreases, whereas it remains relatively unchanged in the critical regions of the curved-tow layers (Fig. 7). The maximum values of K^f_ε in the cross-plied layers were located within the (0/90) laminated joint region, as defined in Fig. 5, and were always greater than the corresponding values in the curved-tow layers. In the curved-tow layers, the greatest values of K^f_ε were near the point of minimum bandwidth of the curved tow. Halving the proportion of cross-plied layers roughly doubles the K^f_ε values in those layers. Hence, the cross-plied layers control the tensile strength of the joint. The curved-tow layers do not contribute substantially to the tensile capability of the grid, as evidenced by the lack of sensitivity of their K^f_ε values to the proportion of curved-tow layers present.

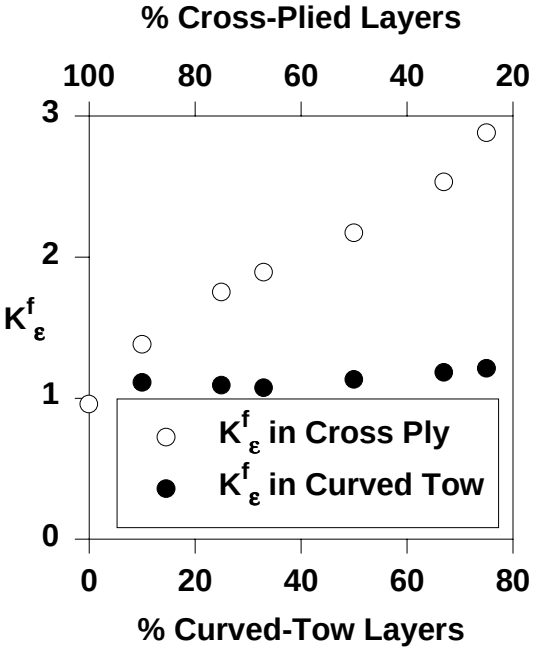

Fig. 7: Maximum fiber strain concentration factor in cross-plied and curved-tow layers as a function of layer proportion

CONCLUSION

Distinct tensile and pullout performance parameters for CFRP grids used as concrete reinforcement result in design tradeoffs for grid mesostructure. The design tradeoffs can be analyzed effectively with the finite element method. Results of an analysis of several novel fiber placement patterns suggest that the proportion of fiber passing straight through the joint governs the stand-alone tensile stiffness and strength of CFRP grids. Pullout stiffness is mostly influenced by the in-plane shear stiffness of the material near the joint rather than the bending resistance of the transverse grid elements. The progressive substitution of tows of fiber that are bent to form continuous networks between the longitudinal and transverse elements progressively degrades the tensile stiffness and through-joint strength of a single longitudinal grid element, but enhances the pullout stiffness due to a beneficial influence on the shear stiffness near the joint. The model results correlated well with experimental results where such comparisons were possible. In the future, a larger, half-symmetry model will be used to more accurately model the pullout process. Results will be applied to beams and

plates reinforced with CFRP grids to determine the best grid design for realistic concrete structures where simultaneous tensile and pullout resistance is required.

ACKNOWLEDGMENTS

The authors gratefully acknowledge the financial support of the National Science Foundation (Grants CMS 9531998 and CMS 9800561, monitored by Dr. John B. Scalzi) and the contribution of materials by Zoltek Corporation and Ashland Chemical Company.

REFERENCES

1. Nanni, A. Ed., Fiber-Reinforced-Plastic for Concrete Structures: Properties and Applications, Elsevier, Amsterdam, 1993.

2. Nanni, A., Bakis, C. E., and Boothby, T. E., "Test Methods for FRP-Concrete Systems Subjected to Mechanical Loads: State of the Art Review," *J. Reinforced Plastics and Composites*, Vol. 14, 1995, pp. 524-588.

3. Engel, R. S., Bakis, C. E., Nanni, A., and Croyle, M. "FRP Grids for Reinforced Concrete: An Investigation of Fiber Architecture," *Proc. Intl. Composites Expo '97*, Soc. Plastics Industry, New York, 1997, pp. 6E.1-6E6.

4. Bakis, C. E., Engel, R. S., Nanni, A., and Croyle, M. G., "FRP Grid Design and Testing," *Proc. FRPRCS-3, Third International Symposium on Non-Metallic (FRP) Reinforcement for Concrete Structures*, Vol. 2, Japan Concrete Institute, Tokyo, Japan, 1997, pp. 591-598.

5. Engel, R. S., Bakis, C. E., Nanni, A., and Croyle, M., "FRP Grid Performance in Concrete Beams: An Investigation of Preform Architecture," *Proc. 2nd International Conference on Composites in Infrastructure*, Vol. II, H. Saadatmanesh and M. R. Ehsani, Eds., 5-7 Jan. 1998, University of Arizona, Tucson, AZ, pp. 80-91.

6. Chamis, C. C., "Simplified Composite Micromechanical Equations for Strength, Fracture Toughness and Environmental Effects," *SAMPE Quarterly*, Vol. 15, 1984, pp. 44-55.

7. Pagano, N. J., in Composite Materials, G. P. Sendeckyj, ed., Vol. 2 of Mechanics of Composite Materials, Academic Press, NY, 1974, pp. 23-44.